Design and Analysis of a Low-profile Microstrip Antenna for 5G Applications using AI-based PSO Approach

Krishanu Kundu[1], Ankan Bhattacharya[2], Firdous H. Mohammed[3], and Narendra Nath Pathak[4]

[1] *G.L. Bajaj Institute of Technology & Management, Greater Noida, India,*
[2] *Hooghly Engineering & Technology College (HETC), Hooghly, West Bengal, India,*
[3] *University of the Cumberland's Williamsburg, Kentucky, USA,*
[4] *Dr. B.C. Roy Engineering College Durgapur, India*

https://doi.org/10.26636/jtit.2023.3.1368

Abstract — Microstrip antennas are high gain aerials for low-profile wireless applications working with frequencies over 100 MHz. This paper presents a study and design of a low cost slotted-type microstrip patch antenna that can be used in 5G millimeter wave applications. This research focuses on the effect of ground slots and patch slots which, in turn, affect different antenna parameters, such as return loss, VSWR, gain, radiation pattern, and axial ratio. The working frequency range varies from 24 to 28 GHz, thus falling within 5G specifications. A subset of artificial intelligence (AI) known as particle swarm optimization (PSO) is used to approximatively solve issues involving maximization and minimization of numerical values, being highly challenging or even impossible to solve in a precise manner. Here, we have designed and analyzed a low-profile printed microstrip antenna for 5G applications using the AI-based PSO approach. The novelty of the research is mainly in the design approach, compactness of size and antenna applicability. The antenna was simulated with the use of HFSS simulation software.

Keywords — 5G applications, high gain, low profile, microstrip patch antenna, PSO

1. Introduction

A low-profile micro strip or patch antenna (MPA) is created by mounting a metal patch plane over the ground level with a dielectric separator between them. Typically, the feed lines and the radiating patch are manufactured of a dielectric substrate using the PCB process. The patch is often square, rectangular, circular, triangular, or elliptical in shape to meet performance-related requirements. For a rectangular patch, length L of the patch is usually in the $0.33\lambda_0 \ldots 0.5\lambda_0$ range, where λ_0 represents the free-space wavelength. The patch must be very thin, hence the thickness of the copper foil used is less than λ_0. The dielectric substrate's height is in the $0.003\lambda_0 \ldots 0.05\lambda_0$ range, while the dielectric constant ranges between 2.2 and 12.

Due to their small size and low profile, microstrip patch antennas have become increasingly popular in smartphones and other consumer electronics devices relying on wireless communications. The benefits of microstrip patch antennas are in their compact size, simple manufacturing methods, low weight, and easy design. This has led to the replacement of traditional antennas used in mobile devices [1]. Selection of the substrate and determination of the patch proportions depend on the operating frequency and on the specification of the dielectric material used. Significant parameters, such as length and width of the patch and substrate, as well as the location and length of the feed network can be estimated employing equations given in [2]–[5]. The available dielectric materials have their unique conduction characteristics and vary in dielectric constants and other parameters that influence the fringing waves in the antenna patch [2]–[5].

Because of the cost factor, the most popular dielectric materials include bakelite, FR4 glass epoxy, Rogers RO4003, Taconic TLC, and Rogers RT/Duroid [6]–[8]. When feeding the signal to the antenna, many techniques, including proximity-coupled, inset feed, aperture-coupled, as well as coaxial probe feed methods, are used [3]–[4], [9].

2. Related Work

Many researchers have used various feeding techniques in recent years to develop MPAs of various shapes and used them in various applications. Sharma proposed, in [10], a small, high gain multiband antenna with a glass-shaped radiating patch and a rectangular ground plane. A unique rectangular-shaped, DGS-based effective multi-band frequency reconfigurable antenna was proposed by Sathikbasha *et al.* in [11]. A portable multi-band MPA with resonances at 23.9, 35.5, and 70.9 GHz, suitable for 5G mobile applications, was demonstrated by Punith *et al.* [12].

A graphene-packed dual band mmWave antenna for 28.1 GHz and 37.4 GHz with a DC bias was proposed by Luo *et al.* [13]. A tiny, portable ultra-wideband microstrip antenna for 5G applications was developed by Araujo *et al.* [14], while a small and dual-polarized triple-band antenna for sub-6 GHz 5G applications was created by Alieldin *et al.* [15].

Naji demonstrated in [16], three fork-shaped monopole-based CPW-fed MPAs: SFA, MFA, and DSFA. Ikram *et al.* [17] presented a MIMO antenna that operates in WLAN (2.45/5.2 GHz), 4G LTE (2.6 GHz), and 5G (24/28 GHz) bands, incorporating a 4-element dual-band and wideband monopole tapered slot system. Parchin *et al.* [18] presented a multi-band slot antenna array for 4G and 5G smartphones, including double element square-ring slot radiators mounted on the PCB corners. Two compact, rectangular, u-shaped parasitic elements-based antennas for 2.6, 6.0, and 8.5 GHz bands have been conceptualized by Asif *et al.* [19]. Such a design is ideal for WiMAX or weather radar applications. A u-shape slotted reconfigurable patch antenna with a low profile and light weight was also shown by Yeole *et al.* [20], while a compact antenna for wideband applications has been proposed by Bhattacharya *et al.* in [21]–[24].

Artificial intelligence (AI) is a field of science in which particle swarm optimization is used [25], [26]. Three main approaches are utilized there [27]: statistical methods, symbolic artificial intelligence, and computational intelligence. Computational intelligence can be implemented using either of the three methods: artificial neural network, fuzzy logic, and evolutionary computation. Swarm intelligence is an active part of evolutionary computation. Just like in the case of ant colony optimization, the working principle of particle swarm optimization (PSO) [28] completely relies on swarm intelligence.

Here, PSO has been applied to optimize the dimensions of a compact sized microstrip antenna. Different iterative structures, namely antennas A–D, have been simulated and optimized using PSO. Finally, we have obtained the D antenna model which is validated by the simulation results and measurements.

3. Antenna Design

In this study, the design is realized by cutting rectangular holes at the patch antenna's radiating edge. That is because slot loading antennas perform better – in terms of resonant frequency, return loss, and bandwidth cost – than a traditional rectangular patch aerial. In the 24 GHz band, the antenna's parameters, such as return loss, VSWR, and radiation pattern have been analyzed, as the decreased bandwidth of microstrip patch antennas is their principal drawback.

The equation for the effective dielectric constant for MPA is [2]:

$$\varepsilon_{reff} = \frac{\varepsilon_r + 1}{2} + \frac{\varepsilon_r - 1}{2}\left[1 + 12\frac{h}{w}\right]^{\frac{1}{2}} . \quad (1)$$

The patch length is stretched on either end by ΔL and can be formulated as [2]:

$$\frac{\Delta L}{h} = 0.412\frac{(\varepsilon_{reff} + 0.3)(\frac{w}{h} + 0.264)}{(\varepsilon_{reff} - 0.258)(\frac{w}{h} + 0.8)} . \quad (2)$$

The effective length of the patch L_{eff} is:

$$L_{eff} = L + 2\Delta L . \quad (3)$$

VSWR is the ratio between the maximum and minimum RF voltage levels in the antenna. The ratio of incident wave and reflected voltage wave amplitudes can be defined as a reflection coefficient ρ, retrieved from:

$$r = \frac{Z_{input} - Z_0}{Z_{input} + Z_0} , \quad (4)$$

where Z_0 is the antenna's characteristic impedance. Reflection coefficient ρ, VSWR and characteristic impedance Z_0 are:

$$\rho = |r| = \frac{VSWR - 1}{VSWR + 1} , \quad (5)$$

$$VSWR = \frac{|r| + 1}{|r| - 1} , \quad (6)$$

$$Z_0 = \sqrt{\frac{L}{C}} , \quad (7)$$

where L signifies inductance and C is the antenna's capacitance. The return loss parameter S_{11} is given by:

$$S_{11} = -20\log\left[\frac{VSWR + 1}{VSWR - 1}\right] , \quad (8)$$

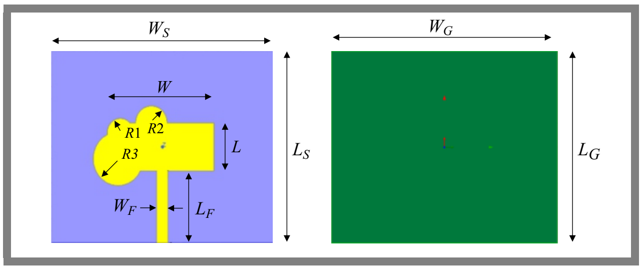

Fig. 1. Reference antenna A a) and ground plane b).

A slot loading antenna outperforms traditional rectangular patch versions in terms of resonance frequency, return loss, and bandwidth. It allows to reduce the aerial's size by more than 60% and lowers resonance frequency by up to 36%. The use of additional slots may contribute to increasing the antenna's bandwidth even further. High gain may by achieved by using a high permittivity substrate and a modified slot shape. This shows that the choice of the substrate and of its thickness is an important design factor. In this research, FR4 substrate is used with its thickness equaling 0.8 mm and its dielectric constant amounting to ε_r of 4.4.

4. PSO in Antenna Design

Particle swarm optimization [29] is a very effective algorithm for solving optimization issues. The given solutions are referred to as "particles", where the best or most appropriate value is referred to as p-best, while g-best refers to the overall best value. The goal is to acquire the best possible p- and g-values for the researched issues. PSO may

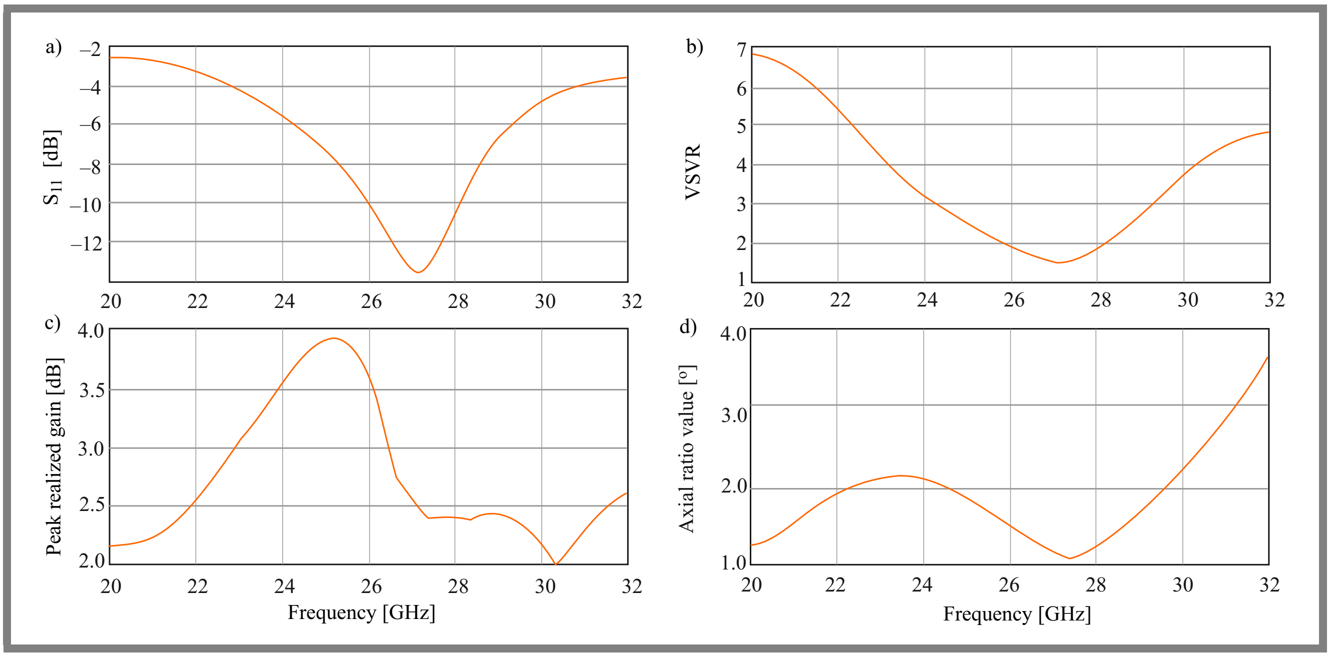

Fig. 2. Antenna A: a) return loss, b) VSWR, c) gain, and d) axial ratio.

be modified in several ways [31], e.g., by replacing the global swarm with several sub-swarms of particles. Such a sub-swarm design aims to mitigate the probability of the PSO algorithm being trapped in a suboptimal solution, which is a useful feature in the design of antenna. Here, PSO is utilized to acquire superior aerial characteristics and to find the best dimensions in order to reduce the return loss as:

$$\min f(x) = \text{ReturnLoss}(x) \text{ subject to } x_l \leqslant x \leqslant x_u \,, \quad (9)$$

Tab. 1. Dimensions of antennas A-D.

Dimension	Value [mm]	Dimension	Value [mm]
Antenna A			
W_S, W_G	10.00	L	2.00
L_S, L_G	8.00	R1	0.58
L_F	3.00	R2, R3	0.70, 1.12
W	4.62	W_F	0.5
Antenna B			
S1	0.08	S8	0.44
S2	0.30	S9	0.18
S3, S13	0.24	S10	0.20
S4	0.38	S11	0.31
S5	0.12	S12	0.19
S6, S7	0.16	S14	0.24
Antenna C			
G1	2.00	G2	2.00
Antenna D			
S15	0.13	S16	0.14

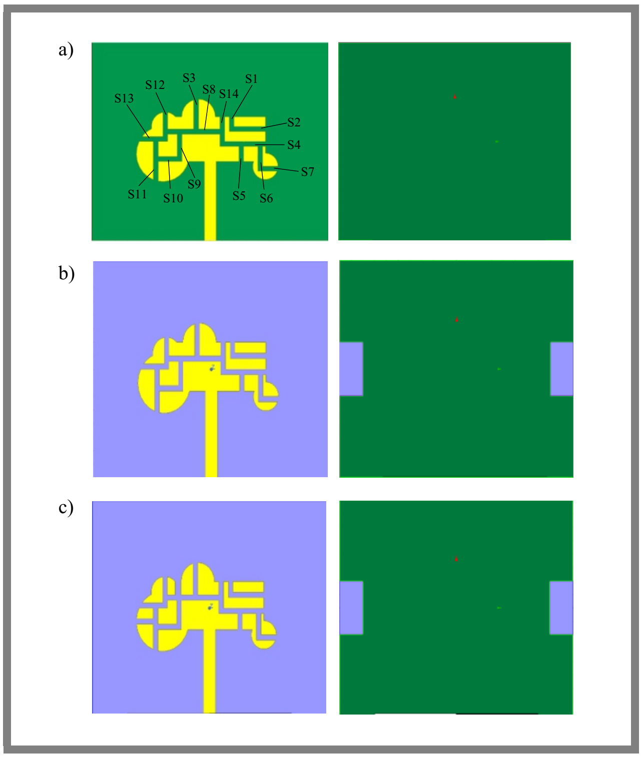

Fig. 3. Patch and ground plane for: a) antenna B, b) antenna C, and c) antenna D.

where x_l and x_u are the minimum and maximum values of MPA dimensions (length and width), respectively. For PSO optimization the following parameters were used:

- number of variables = 2 (L, W),
- acceleration factors = 2, 2,
- number of iterations= 1000,
- population size = 100.

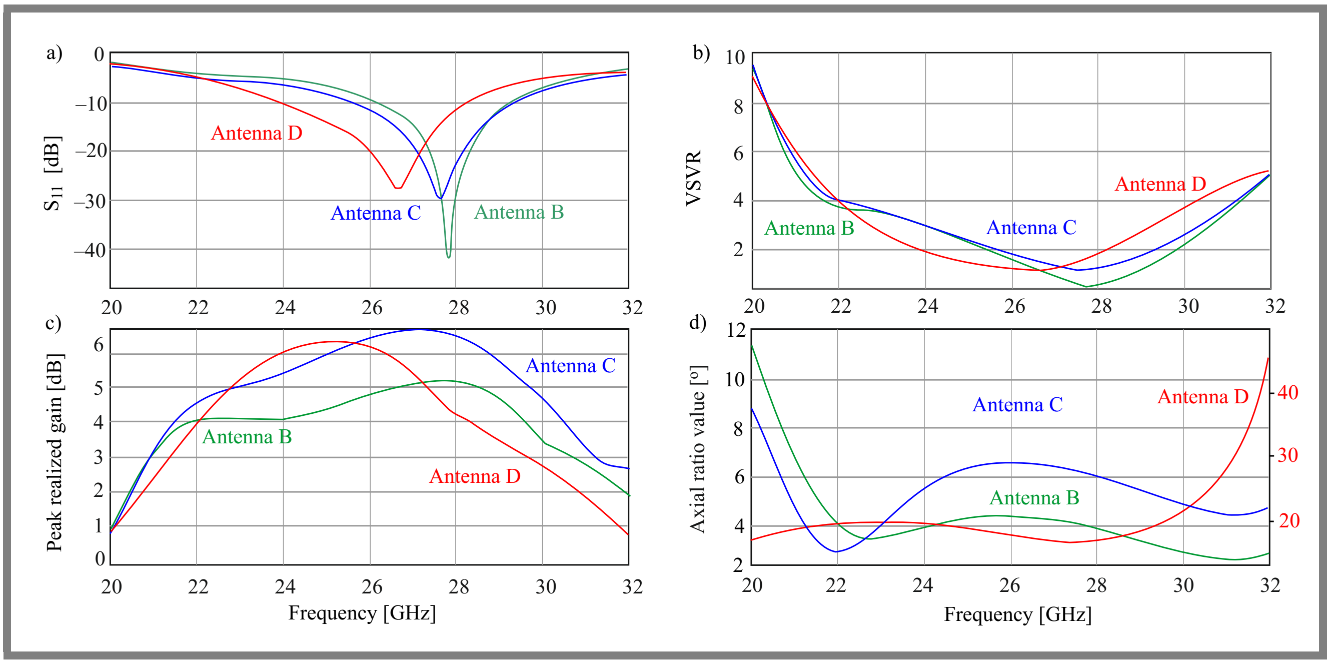

Fig. 4. Return loss a), VSWR b), gain c), and axial ratio d) for antennas B, C, D.

5. Antenna Simulation

The initial reference design is named as antenna A (see Fig. 1) and the dimensions of this design are presented in Tab. 1. The assumed initial dimensions offer a gain of 2.5 dB, return loss S_{11} of $\geqslant$ 30 dB at approx. 27 GHz, VSWR = 1.5 (Fig. 2a-c). However, the axial ratio does not meet the requirement of being lower than 3 dB (Fig. 2d). Therefore, further improvements are required.

In the next iteration (antenna B), slots have been introduced to the design and a new structure was created, as shown in Fig. 3a, Tab. 1. Simulation results presented in Fig. 4 (green curve) show that the slots have affected the axial ratio, the S_{11} has shifted towards 28 GHz with VSWR = 1. The frequency band with a high gain of approx. 4 dB is wider than for antenna A. Further modifications aim to create a version with an even higher gain (antenna C, Fig. 3b, and Tab. 1). Simulation results presented in Fig. 4 (blue curve) show that antenna C is characterized by a return loss of $\geqslant$ 45 dB, VSWR of 1, gain of 6 dBi and a bandwidth of 3.2 GHz. Due to the slots present on the ground plane, a narrow band has been achieved with a minimum S_{11} value near 28 GHz.

To increase gain even more, another design was developed, referred as antenna D (Fig. 3c, Tab. 1). From the simulations we can conclude that for antenna D, the return loss equals $\geqslant$ 40, with VSWR of 0.8 (Fig. 4, red curve) and the gain reached 6.6 dB. An acceptable change has been observed in the axial ratio and a wide bandwidth of 4 GHz. Table 2 shows the comparison of parameters of all simulated antennas (A to D) while Fig. 5 shows the evolution of the patch for A–D prototypes.

Tab. 2. Comparison of specific antenna designs.

Antenna	Return loss S11	VSWR	Bandwidth	Gain
A	$\geqslant$ 30	1.5	2.1 GHz	2.5 dB
B	$\geqslant$ 33	1	3.0 GHz	4 dB
C	$\geqslant$ 45	1	3.2 GHz	6 dB
D	$\geqslant$ 40	0.8	4.0 GHz	6.6 dB

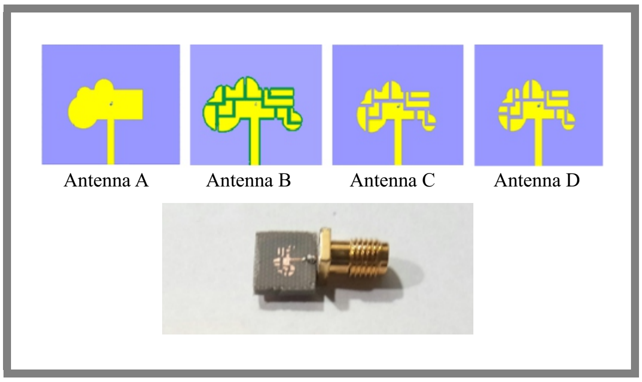

Fig. 5. Antenna design evolution (A to D) and fabricated prototype.

6. Antenna Fabrication and Measurements

To verify the simulation data, the designed antennas were fabricated and the return losses were measured using a vector network analyzer (VNA). Figure 6 shows the the value of the return loss parameter for all four prototypes.

7. Conclusions

In this work, the effects of changing the dimensions of ground slots, as well as the patch of a 5G microstrip antenna [31], [32],

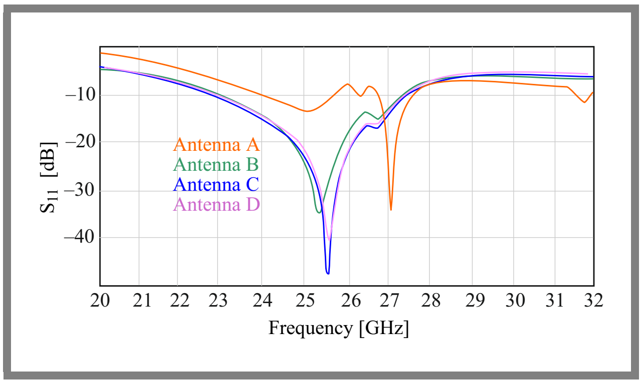

Fig. 6. Return loss of: a) antenna A, b) antenna B, c) antenna C, and d) antenna D.

impacting the different parameters of the antenna, have been analyzed. The proposed antenna is designed using the PSO approach and uses the low-cost and widely available FR4 substrate. It offers a high gain of 6.6 dB with a return loss $|S_{11}|$ parameter of over 40 dB at 27 GHz. Post-optimization of the design using the PSO technique has resulted in a compact structure with minimal dimensions.

References

[1] J. Howell, "Microstrip Antennas", *IEEE Transactions on Antennas and Propagation*, vol. 23, no. 1, pp. 90–93, 1975 (https://doi.org/10.1109/TAP.1975.1141009).

[2] C.A. Balanis, "Antenna Theory: a Review", *Proceedings of the IEEE*, vol. 80, no. 1, pp. 7–23, 1992 (https://doi.org/10.1109/5.119564).

[3] C.A. Balanis, *Antenna Theory: Analysis and Design*, 3rd ed. Wiley, 848 p., 2005 (ISBN: 9780470576649).

[4] G. Kumar and K.P. Ray, *Broadband Microstrip Antennas*, 1st ed. Artech, 451 p., 2002 (ISBN: 9781580537674).

[5] P. Upender, P.A.H. Vardhini, and V. Prakasam, "Performance Analysis and Development of Printed Circuit Microstrip Patch Antenna with Proximity Coupled Feed at 4.3 GHz (C-band) with Linear Polarization for Altimeter Application", *International Journal of Computing and Digital Systems*, vol. 10, no. 1, 2020 (https://dx.doi.org/10.12785/ijcds/1001116).

[6] O. Barrou, A. El Amri, and A. Reha, "Comparison of Feeding Modes for a Rectangular Microstrip Patch Antenna for 2.45 GHz Applications", *Lecture Notes in Electrical Engineering*, vol. 397, pp. 457–469, 2016 (https://doi.org/10.1007/978-981-10-1627-1_36).

[7] A.K. Khan, T.A. Shaem, and M.A. Alim, "Graphene Patch Antennas with Different Substrate Shapes and Materials", *Optik*, vol. 202, art. no. 163700, 2020 (https://doi.org/10.1016/j.ijleo.2019.163700).

[8] G. Kaur *et al.*, "Performance analysis of conductive patch materials for the design and fabrication of microstrip patch antennas", in: 2017 *Progress in Electromagnetics Research Symposium*, St. Petersburg, Russia, 2017 (https://doi.org/10.1109/piers.2017.8261793).

[9] A. Khan and R. Nema, "Analysis of Five Different Dielectric Substrates on Microstrip Patch Antenna", *International Journal of Computer Applications*, vol. 55, no. 14, pp. 40–47, 2012 (https://doi.org/10.5120/8826-2905).

[10] M. Sharma, "Design and Analysis of Multi-band Antenna for Wireless Communication", *Wireless Personal Communications*, vol. 114, no. 2, pp. 1389–1402, 2020 (https://doi.org/10.1007/s11277-020-07425-9).

[11] M.J. Sathikbasha and V. Nagarajan, "Design of Multi-band Frequency Reconfigurable Antenna with Defected Ground Structure for Wireless Applications", *Wireless Personal Comm.*, vol. 113, no. 2, pp. 867–892, 2020 (https://doi.org/10.1007/s11277-020-07256-8).

[12] S. Punith, S.K. Praveenkumar, A.A. Jugale, and M.R. Ahmed, "A Novel Multi-band Microstrip Patch Antenna for 5G Communications", *Procedia Computer Science*, vol. 171, pp. 2080–2086, 2020 (https://doi.org/10.1016/j.procs.2020.04.224).

[13] Y. Luo *et al.*, "Graphene-based dual-band antenna in the millimeter-wave band", *Microwave and Optical Technology Letters*, vol. 60, no. 12, pp. 3014–3019, 2018 (https://doi.org/10.1002/mop.31435).

[14] H.X. Araujo, A.E. Freitas, D.N. Prata, I.R.S. Casella, and C.E. Capovilla, "Multi-band Antenna Design Comprising the Future 5G Mobile Technology", *Electrotechnical Review*, vol. 95, no. 2, pp. 108–111, 2019 (https://doi.org/10.15199/48.2019.02.25).

[15] A. Alieldin *et al.*, "A Triple-Band Dual-Polarized Indoor Base Station Antenna for 2G, 3G, 4G and Sub-6 GHz 5G Applications", *IEEE Access*, vol. 6, pp. 49209–49216, 2018 (https://doi.org/10.1109/access.2018.2868414).

[16] D.K. Naji, "Design of Compact Dual–band and Tri-band Microstrip Patch Antennas", *International Journal of Electromagnetics and Applications*, vol. 8, no. 1, pp. 26–34, 2018 (https://doi.org/10.5923/j.ijea.20180801.02).

[17] M. Ikram, N. Nguyen–Trong, and A. Abbosh, "Multi-band MIMO Microwave and Millimeter Antenna System Employing Dual-Function Tapered Slot Structure", *IEEE Transactions on Antennas and Propagation*, vol. 67, no. 8, pp. 5705–5710, 2019 (https://doi.org/10.1109/tap.2019.2922547).

[18] N.O. Parchin *et al.*, "Multi-Band MIMO Antenna Design with User-Impact Investigation for 4G and 5G Mobile Terminals", *Sensors*, vol. 19, no. 3, art. no. 456, 2019 (https://doi.org/10.3390/s19030456).

[19] S. Asif *et al.*, "A Compact Multi-band Microstrip Patch Antenna with U-shaped Parasitic Elements", in: *2015 IEEE International Symposium on Antennas and Propagation & USNC/URSI National Radio Science Meeting*, Vancouver, Canada, 2015 (https://doi.org/10.1109/aps.2015.7304695).

[20] D.S. Yeole and U.P. Khot, "Reconfigurable Multi-band Microstrip Patch Antenna Design for Wireless Communication Applications", in: *2016 IEEE International Conference on Recent Trends in Electronics, Information & Communication Technology (RTEICT)*, Bangalore, India, 2016 (https://doi.org/10.1109/rteict.2016.7807899).

[21] A. Bhattacharya, B. Roy, R.F.S. Caldeirinha, and A.K. Bhattacharjee, "Low-profile, Extremely Wideband, Dual-band–notched MIMO Antenna for UWB Applications", *International Journal of Microwave and Wireless Technologies*, vol. 11, no. 7, pp. 719–728, 2019 (https://doi.org/10.1017/S1759078719000266).

[22] A. Bhattacharya, B. Roy, S.K. Chowdhury, and A.K. Bhattacharjee, "Computational and Experimental Analysis of a Low-profile, Isolation-enhanced, Band-notch UWB–MIMO Antenna", *Journal of Computational Electronics*, vol. 18, no. 2, pp. 680–688, 2019 (https://doi.org/10.1007/s10825-019-01309-3).

[23] A. Bhattacharya, B. Roy, S.K. Chowdhury, and A.K. Bhattacharjee, "A Compact Fractal Monopole Antenna with Defected Ground Structure for Wideband Communication", *Applied Computational Electromagnetics Society Journal*, vol. 33, no. 3, pp. 347–350, 2018 (ISSN: 10544887).

[24] A. Bhattacharya, B. Roy, S.K. Chowdhury, and A.K. Bhattacharjee, "Design and Analysis of a Koch Snowflake Fractal Monopole Antenna for Wideband Communication", *Applied Computational Electromagnetics Society Journal*, vol. 32, no. 6, 2017 (ISSN: 10544887).

[25] N. Behnia, M. Zare, V. Moosavi, and S.J. Khajeddin, "An intercomparison of Different PSO-Optimized Artificial Intelligence Algorithms for Thermal-based Soil Moisture Retrieval", *Earth Science Informatics*, vol. 15, no. 11, pp. 473–484, 2022 (https://doi.org/10.1007/s12145-021-00747-7).

[26] V. Chourasia, S. Pandey, and S. Kumar, "Optimizing the Performance of Vehicular Delay Tolerant Networks Using Multi-objective PSO and Artificial Intelligence", *Computer Communications*, vol. 177, pp.

10–23, 2021 (https://doi.org/10.1016/j.comcom.2021.06.006).

[27] S. Zhao, W. Xu, and L. Chen, "The Modeling and Products Prediction for Biomass Oxidative Pyrolysis Based on PSO–ANN Method: an Artificial Intelligence Algorithm Approach", *Fuel*, vol. 312, art. no. 122966, 2022 (https://doi.org/10.1016/j.fuel.2021.122966).

[28] A.G. Gad, "Particle Swarm Optimization Algorithm and its Applications: a Systematic Review", *Archives of Computational Methods in Engineering*, vol. 29, no. 12, pp. 2531–2561, 2022 (https://doi.org/10.1007/s11831-021-09694-4).

[29] J. Kennedy and R. Eberhart, "Particle Swarm Optimization", in *Proc. of IEE International Conference on Neural Networks*, vol. 4, pp. 1942–1948, 1995 (https://doi.org/10.1109/ICNN.1995.488968).

[30] K. Sharma and G.P. Pandey, "Pattern Correction in Planar Antenna Array Using Multi–objective Particle Swarm Optimization and Continuous Excitation", *Iranian Journal of Science and Technology, Transactions of Electrical Engineering*, vol. 45, no. 2, pp. 367–380, 2021 (https://doi.org/10.1007/s40998-020-00378-6).

[31] K. Sharma, "Investigations of Microstrip Antenna Using Machine Learning", *Ph.D. Thesis*, Pandit Deendayal Energy University, Gandhinagar, 2021 (http://ir.pdpu.ac.in:8080/xmlui/handle/123456789/102).

[32] A. Bhattacharya and S. Pal, "An Extremely Compact and Low-Cost Antenna Sensor Designed for IoT-Integrated Biomedical Applications", in *Internet of Things and Data Mining for Modern Engineering and Healthcare Applications*, pp. 261–268, Chapman and Hall/CRC, 2022 (https://doi.org/10.1201/9781003217398).

Krishanu Kundu, Ph.D.
Department of Electronics and Communication Engineering
https://orcid.org/0000-0003-1057-4713
E-mail: krishanukundu08@gmail.com
G.L. Bajaj Institute of Technology & Management, Greater Noida, India
https://www.glbitm.org

Ankan Bhattacharya, Ph.D.
Department of Electronics and Communication Engineering
https://orcid.org/0000-0003-2350-1687
Hooghly Engineering & Technology College (HETC), Hooghly, West Bengal, India
https://www.hetc.ac.in

Firdous H. Mohammed, Ph.D. Scholar
Computer Information System
University of the Cumberland's Williamsburg, Kentucky, USA
https://www.ucumberlands.edu

Narendra Nath Pathak, Ph.D.
Department of Electronics and Communication Engineering
https://orcid.org/0000-0002-5670-3229
Dr. B.C. Roy Engineering College Durgapur, India
https://bcrec.ac.in